HHS Public Access

Author manuscript

Genes Immun. Author manuscript; available in PMC 2011 January 01.

Published in final edited form as:

Genes Immun. 2010 July ; 11(5): 384–396. doi:10.1038/gene.2010.27.

Variations in Gnai2 and Rgs1 Expression Affect Chemokine Receptor Signaling and the Organization of Secondary Lymphoid Organs

Il-Young Hwang[1], **Chung Park**[1], **Kathleen Harrision**[1], **Ning-Na Huang**[1], and **John H. Kehrl**[1,2]

[1] B-Cell Molecular Immunology Section, Laboratory of Immunoregulation, National Institute of Allergy and Infectious Diseases, National Institutes of Health, Bldg 10, Room 11N214, 10 Center Dr. MSC 1876, Bethesda, MD 20892-1876

Abstract

Ligand bound chemoattractant receptors activate the heterotrimeric G protein Gi to stimulate downstream signaling pathways to properly position lymphocytes in lymphoid organs. Here we show how variations the expression of a chemokine receptor and in two components in the signaling pathway, $G\alpha_{i2}$ and RGS1, affects the output fidelity of the signaling pathway. Examination of B cells from mice with varying numbers of intact alleles of Ccr7, Rgs1, Gnai2, and Gnai3 provided the basis for these results. Loss of a single allele of either Gnai2 or Rgs1 affected CCL19 triggered chemotaxis, while loss of a single allele of Ccr7, which encodes the cognate CCL19 receptor, had little effect. Emphasizing the importance of Gnai2, B cells lacking Gnai3 expression responded to chemokines better than did wild type B cells. At an organismal level, variations in Rgs1 and Gnai2 expression affected marginal zone B cell development, splenic architecture, lymphoid follicle size, and germinal center morphology. Gnai2 expression was also needed for the proper alignment of MOMA-1^+ macrophages and MAdCAM-1^+ endothelial cells along marginal zone sinuses in the spleen. These data indicate that chemoattractant receptors, heterotrimeric G-proteins, and RGS protein expression levels have a complex inter-relationship that affects the responses to chemoattractant exposure.

Keywords

heterotrimeric G protein; RGS protein; chemotaxis; calcium flux; spleen; marginal zone

Introduction

Chemoattractants help recruit and position lymphocytes and dendritic cells in lymphoid organs and inflammatory sites.[1–3] Most lymphocyte chemoattractants and chemokines signal through G-protein coupled receptors that use the heterotrimeric G-protein Gi to activate downstream effectors[3]. The binding of ligand activates receptors triggering $G_{\alpha i}$ subunits to exchange GTP for GDP resulting in the dissociation of the Gα subunit from its

[2]Corresponding author. Dr. John H. Kehrl, Phone 301-443-6907; Fax: 301-402-0070; jkehrl@niaid.nih.gov.

associated $G_{\beta\gamma}$ heterodimer. The release of Gi associated Gβγ subunits is necessary for triggering directional migration.[4,5] Since G_{α} subunits possess an intrinsic GTPase activity, GTP hydrolysis leads to the re-assembly of heterotrimeric G-protein causing signaling to cease.[6,7] Lymphocytes express two members of the Gα subfamily, $G\alpha_{i2}$ and $G\alpha_{i3}$[8,9] *Gnai3*$^{-/-}$ mice were reportedly without a phenotype,[10] however, more recently a defect in the early seeding of the thymus by progenitors has been observed.[11] *Gnai2*$^{-/-}$ mice exhibit defective lymphocyte chemokine receptor signaling as evidenced by depressed chemotaxis, defective homing to lymph nodes, poor adherence to lymph node high endothelial venules, and decreased motility within lymph node follicles.[8,9]

G protein-coupled receptors (GPCRs) such as chemokine receptors exist in multiple dynamic states including ligand-bound, inactive, and G protein-coupled, which influence G protein activation and subsequent downstream signaling. A recent study used parameter variation and sensitivity analysis to examine the ligand- and cell-specific parameters, which determine cellular responses in a dynamic model of GPCR signaling.[12] Not surprisingly, the most important factor was the ability of the ligand to trigger an active receptor conformation, but in addition, several cell-specific parameters strongly correlated with G-protein activation. The three most important in rank order were G-protein concentration, Gα GTPase activity, and receptor expression.[12] Notably; these results indicate that the expression of a GPCR or G protein several-fold above or below endogenous levels could result in responses inconsistent with those measured in endogenous systems, thereby providing a caveat for the interpretation of results from transfection studies. Also, small variations in cell-specific parameters may actually change a ligand-induced positive response to a negative one.[12]

Because of the ease of assessing chemokine receptor expression by flow cytometry immunologists have focused on those levels as a measure of chemokine responsiveness largely ignoring two other potentially important cell-specific parameters, G-protein levels and Gα GTPase activity, the later which largely depends on the presence of RGS proteins in the system.[13] Increasingly attention has been focused on RGS proteins as a new class of pharmaceutical targets.14 In this study we examined the consequences of altering $G\alpha_{i2}$ and RGS1 levels on B cell responses to three different chemokines CXCL12, CXCL13, and CCL19 by using B cells from mice with one or two disrupted alleles of *Rgs1* or *Gnai2* and from mice that have various combinations of disrupted and wild type alleles of these two genes.[8,15] In addition we compared the responsiveness of B cells from wild type mice to those with only one intact allele of *Ccr7*. Our results indicate that the RGS1/$G\alpha_{i2}$ ratio is an important parameter to consider in assessing B cell chemokine responsiveness. They also provide some insights into the role of G-protein signaling in the organization of the splenic lymphoid architecture.

Results

The generation of mice for analysis and the impact of genotype on early mouse viability

On a C57BL/6 background the *Rgs1*$^{-/-}$ mice bred and thrived similar to wild type mice while the *Gnai2*$^{-/-}$ mice bred poorly or not at all and were maintained as heterozygotes. Litters from heterozygotic crosses generated lower than expected numbers of *Gnai2*$^{-/-}$ mice.

A previous study had reported that *Gnai2*$^{+/-}$ intercrosses produced 9.7% *Gnai2*$^{-/-}$ mice versus the expected 25%. A significant loss of *Gnai2*$^{-/-}$ mice was reported to occur perinatally.[16] In our colony *Gnai2*$^{-/-}$ mice are smaller than their wild type littermates and often die prior to 6 months of age of varying causes. The *Gnai3*$^{-/-}$ mice we have used have been backcrossed 3–6 generations onto C57BL/6 background and have thrived normally. Double heterozygote crosses were bred to generate mice with the varying alleles of *Rgs1* and *Gnai2*. The double knock-out mice exhibited the same smaller stature as did the *Gnai2*$^{-/-}$ mice (Figure 1). Analysis of the frequency of the different genotypes obtained from these crosses revealed an increased representation of the wild type *Gnai2* allele in the offspring. The most over represented genotype among the mice was *Rgs1*$^{+/-}$/*Gnai2*$^{+/+}$ while the *Rgs1* allele status had little effect on the survival of the mice lacking both *Gnai2* alleles. There was also the suggestion that the lack of one allele of *Gnai2* negatively impacted the survival of the mice.

Varying levels of Gnai2 and Rgs1 expression affected B cell responses to chemokines

In lymphocytes the loss of a single allele of *Gnai2* reduced $G\alpha_{i2}$ levels approximately 50% while $G\alpha_{i3}$ levels increased a similar amount. A loss of both alleles of *Gnai2* resulted in a several fold increase in $G\alpha_{i3}$ levels compared to controls.[8] The loss of *Gnai3* has been reported to not significantly impact $G\alpha_{i2}$ expression levels[17] and the *Gnai3*$^{-/-}$ lymphocytes we used had similar $G\alpha_{i2}$ expression as did littermate controls (data not shown). The disruption of a single allele of *Rgs1* reduced *Rgs1* mRNA expression 50% (data not shown). To determine the relative importance of *Gnai2* and *Rgs1* expression on chemokine receptor signaling in B lymphocytes, we prepared splenic B cells from mice with various disrupted alleles of *Gnai2* and *Rgs1* and tested them using standard chemotaxis assays to CXCL12, CCL19, and CXCL13. The specific migration to three different concentrations of chemokine was measured. We found that loss of one allele of *Rgs1* increased responses to all three chemokines and the loss of a second allele further increased the specific migration of B lymphocytes (Figure 2). In contrast the loss of a single allele of *Gnai2* reduced responsiveness and the additional loss of an *Rgs1* allele improved the response. The B cells from the double knock-out mice responded somewhat better than did the *Gnai2*$^{-/-}$ mice arguing that the loss of *Rgs1* partially compensated for the loss of *Gnai2* (Figure 2). This is inconsistent with the known functional role of RGS1 as a $G\alpha_{i2}$ GAP. Since RGS1 is also a Gq_{α} GAP[18] lymphocyte chemokine receptors may couple to Gq in the absence of $G\alpha_{i2}$, which would explain the enhanced response in the absence of *Rgs1*. Gq has been shown to couple to certain chemoattractant receptors in neutrophils and dendritic cells.[19]

Exposure of B lymphocytes elicits a rapid increase in intracellular calcium $[Ca^{2+}]_i$ which is mediated by $G\beta\gamma$ stimulation of phospholipase β and blocked by pre-treatment with pertussis toxin. Although the increase in $[Ca^{2+}]_i$ apparently contributes little to lymphocyte chemotaxis, it provides an easy and rapidly accessible measure of heterotrimeric G-protein activation. Therefore, we examined chemokine induced changes in $[Ca^{2+}]_i$ using B cells from the various mouse strains. We found that the loss of one allele of *Rgs1* enhanced the $[Ca^{2+}]_i$ response to CXCL12 and CXCL13, both the peak level and duration, while the loss of both alleles resulted in a further increase (Figure 3). In contrast to previous experiments with T cells where the loss of one allele of *Gnai2* substantially decreased CXCL12 induced

increase in $[Ca^{2+}]_I$,[9] the loss of one allele in B cells had little effect on the CXCL12 induced increase in $[Ca^{2+}]_i$ although the CXCL13 induced response was impaired. Similar to T cells the loss of both alleles of *Gnai2* in B cells severely compromised the CXCL12 induced increases in $[Ca^{2+}]_i$ and as well the CXCL13 triggered response. The double heterozygotic B cells had a phenotype most similar to the mice that lacked an *Rgs1* allele and the double knock-out mice had a surprisingly good $[Ca^{2+}]_i$ response, a result consistent with a partial re-coupling to Gq. Together these results indicate that in B lymphocytes chemokine receptor signaling induced changes in $[Ca^{2+}]_i$ and chemotaxis are sensitive to changes in $G\alpha_{i2}$ and RGS1 expression.

To specifically examine the relationship between chemokine dose and intracellular signaling in B cell lacking *Rgs1* we stimulated B cells purified from wild type and *Rgs1*$^{-/-}$ mice with increasing concentrations of CXCL12 or CXCL13 and plotted the log of the concentration versus the peak in $[Ca^{2+}]_i$. For both chemokines we found that at each concentration the peak response of the *Rgs1*$^{-/-}$ B cells exceeded that of wild type mice and the difference became more evident at higher concentrations. Similar results were observed with a human B cell line, where RGS1 and RGS13 expression were reduced, and with an immature human mast cell line, where RGS13 expression was reduced.[20;21]

B cells from Gnai3 deficient mice had enhanced responses to chemokines

B and T lymphocyte chemotaxis, lymph nodes homing, lymph node egress, thymus egress, and positioning within lymph node organs are all sensitive to pertussis toxin treatment, which ADP ribosylates the $G\alpha_i$ subunits $G\alpha_{i1}$, $G\alpha_{i2}$, $G\alpha_{i3}$, and Go_α but not Gz_α. Mature B and T lymphocytes predominantly express $G\alpha_{i2}$ and $G\alpha_{i3}$, but not $G\alpha_{i1}$. Lymphocytes lacking $G\alpha_{i2}$ exhibit defects in all of the above with the exception of lymph node and thymus egress although sphingosine 1-phosphate (S1P) mediated lymphocyte chemotaxis is markedly reduced in the absence of $G\alpha_{i2}$.8,9,22. Some residual chemotaxis has been noted with the *Gnai2*$^{-/-}$ lymphocytes, however, it is insensitive to pertussis toxin treatment.[8,9] Together these data argue that $G\alpha_{i3}$ cannot mediate lymphocyte CXCR4, CXCR5, or CCR7 triggered chemotaxis. The inability of $G\alpha_{i3}$ to substitute for $G\alpha_{i2}$ in lymphocyte chemotaxis despite the elevated $G\alpha_{i3}$ expression is somewhat surprising. To directly examine the role of $G\alpha_{i3}$ in B lymphocytes we performed chemotaxis assays and examined chemokine induced changes in $[Ca^{2+}]_i$ using B cells prepared from *Gnai3*$^{-/-}$ mice. The percentage of chemokine-responsive cells from the *Gnai3*$^{-/-}$ mice equaled or exceeded the number from controls (Figure 4). In addition the increase in $[Ca^{2+}]_i$ elicited by the CXCL12, CXCL13, and CCL19 exceeded the levels achieved with wild type control B cells (Figure 4). These results indicate that in contrast to $G\alpha_{i2}$, $G\alpha_{i3}$ is not needed for B lymphocytes to respond to chemokines, and that in its absence, $G\alpha_{i2}$ may more efficiently couple to chemoattractant receptors.

Loss of single allele of Ccr7 minimally affected CCR7 triggered chemotaxis of B cells

Since we had observed changes in chemokine responsiveness in B cells lacking one allele of *Rgs1* or one allele of *Gnai2* we examined the consequences of the loss of one allele of *Ccr7* on B cell responsiveness to the chemoattractant Ccl19. Varying *Ccr7* expression, hence Ccr7 mediated signaling, is known to help B cells position themselves properly in the B cell

follicle.[23] We isolated B cells from wild type, *Ccr7*$^{+/-}$, and *Ccr7*$^{-/-}$ littermates derived from a heterozygote cross and tested for their ability to respond in a standard chemotaxis assay. Surprisingly we found that the lack of one allele of *Ccr7*, which caused a greater than 50% reduction in CCR7 expression as assessed by flow cytometry, had only a modest impact of B cell chemotaxis to the Ccl19. B cells from *Ccr7*$^{+/-}$ mice responded to low concentrations of CCL19 as well as did the wild type control mice although they showed a modest decrease (20%) at higher concentrations of CCL19 (Figure 5). As expected B cells from *Ccr7*$^{-/-}$ mice failed to respond to CCL19, but they responded well to CXCL12 even surpassing the wild type B cell responses particularly with lower concentrations of chemokine. In addition, the *Ccr7*$^{-/-}$ B cells responded better to CXCL13 than did the wild type B cells (data not shown). Thus, the lack of one allele of *Rgs1* or *Gnai2* affected *Ccl19* triggered chemotaxis more than did the loss of a single allele of *Ccr7*. This argues that small changes in chemokine receptor expression may not be translated into significant changes in chemokine responsiveness while similar magnitude changes in *Gnai2* and *Rgs1* expression can impact chemokine responsiveness.

Varying levels of Gnai2 and Rgs1 affected marginal zone B cell development and the splenic architecture

Previous results had indicated that *Gnai2*$^{-/-}$ mice had reduced number of marginal zone B cells[24] while *Rgs1*$^{-/-}$ mice had increased numbers of marginal zone B cells.[25] To examine the interaction between *Rgs1* and *Gnai2* in the marginal zone B cell development, we first determined the numbers of follicular, transitional, and marginal zone B cells in wild type mice and mice that had varying numbers of intact *Gnai2* and *Rgs1* alleles and in *Gnai3*$^{-/-}$ mice (Table 1). Disruption of one allele of *Rgs1* increased the number of marginal zone B cells and loss of the second allele further increased them resulting in approximately twice as many B220, CD21^{high}, CD23^{-} B cells as in the wild type mice. Loss of a single allele of Gnai2 did not affect the number of B220, CD21^{high}, CD23− B cells, but loss of both alleles reduced the number of marginal zone B cells by one-half. The double heterozygote resembled the *Rgs1* heterozygote suggesting that the number of marginal zone B cells is more sensitive to *Rgs1* expression than *Gnai2*. In contrast to the lack of *Gnai2*, the loss of *Gnai3* did not affect the number of marginal zone B cells.

Next, we used immunohistochemistry to examine the spleens of the different mice. B220 versus CD3 staining revealed that the spleens of the *Rgs1*$^{-/-}$ mice contained prominent follicles with expanded B cell zones relative to the T cell zone while the *Gnai2*$^{-/-}$ ice had a reduction in splenic follicles and those present were small with poorly developed B cell zones. Scattered throughout the spleen were areas of loosely organized B and T cells. The B220/CD3 immunohistochemistry with the double knock-out spleens appeared similar to those from the *Gnai2*$^{-/-}$ mice although the overall splenic architecture was even more disrupted. While the sections from the double heterozygotes appeared most similar to those from the wild type mice the distinction between B and T cell zones was not as sharp as that in the wild type mice and the follicles were smaller (Figure 6a). To assess spontaneous germinal centers we analyzed the expression of B220 versus peanut agglutinin (PNA) staining in the various sections. The spleen sections from the *Rgs1*$^{-/-}$ mice had 6 fold more spontaneous germinal centers compared to those from wild type mice (Figure 6b-d). While

the *Gnai2*$^{-/-}$ mice had fewer spontaneous germinal centers, the double knock-out had more than did the wild type mice despite the severe disorganization of their splenic architecture. The double heterozygotic mice spleens had more prominent germinal centers than did those from wild type mice. The average number of germinal centers per spleen section from the different genotype mice was as follows: 7.0+/−2.1 wild type; 4.4+/−1.9 *Gnai2*$^{-/-}$, 36+/−4.4 *Rgs1*$^{-/-}$, 19.7+/−3.4 *Rgs1*$^{+/-}$*Gnai2*$^{+/-}$, and 21+/−3.1 *Rgs1*$^{-/-}$ *Gnai2*$^{-/-}$. To assess the organization of germinal center light and dark zones, we examined the expression of IgD versus CD35 (Figure 6c) using the splenic sections from the different genotypes. CD35 recognizes CR1/2 and identifies follicular dendritic cells (FDC) in the primary and secondary follicles and reacts with FDCs in the germinal center light zone.[26] The constitutive germinal centers present in the spleens of wild type mice were small with poorly developed dark zones. In contrast in the *Rgs1*$^{-/-}$ mice the splenic germinal centers were often large with prominent dark zones. The germinal centers from the double knock-out and *Gnai2*$^{-/-}$ mice were disorganized with a poor segregation of the light and dark zones. The germinal center organization in double heterozygotic mice was largely intact.

To assess the splenic marginal zone region in the various mice, we analyzed sections immunostained for MAdCAM-1 and CD1d; MOMA-1 and CD1d; and IgD and IgM[27]. In wild type spleens the MAdCAM-1+ cells were tightly cohesive in a thin layer encircling the follicle, however, in the spleens from the *Gnai2*$^{-/-}$ mice and the double knock-out mice this thin layer was dispersed. In addition in these same mice the number of CD1d^{+} cells was sharply reduced (Figure 7a). The morphology of the marginal zone sinus was intact in the sections from the *Rgs1*$^{-/-}$ mice and from the double heterozygotes (Figure 7a). Consistent with that result the MOMA-1^{+} cells were tightly associated with MAdCAM-1^{+} cells in the wild type mice, *Rgs1*$^{-/-}$ and double heterozygote mice, but were no longer so in the sections from the *Gnai2*$^{-/-}$ and double knock-out mice (Figure 7b). Examination of IgM versus IgD Immunostaining also demonstrated significant abnormalities in the spleens from the *Rgs1*$^{-/-}$, *Gnai2*$^{-/-}$, and double knock-out mice while the spleens from the double heterozygotes were more normal appearing (Figure 7c). The spleens from the *Rgs1*$^{-/-}$ mice had an increased number of IgM high cells both within the marginal zone and in the follicle. The spleens from the *Gnai2*$^{-/-}$ and double knock-out mice had a markedly disordered marginal zone with an increased number of IgM high cells interspersed among the follicular B cells. Together these data suggest that the ratio between RGS1/Gα_{i2} affects the integrity of the lymphoid architecture, spontaneous germinal center formation, and the frequency of marginal zone B cells. In addition Gα_{i2} is crucial for normal development of the marginal sinus in the spleen.

Discussion

The above findings aid our understanding of how the variation in the expression of signaling molecules affects the responses of lymphocytes to environmental cues. Modest changes in the ratio between an RGS protein and a Gα_i subunit modulates the responsiveness of B lymphocytes to chemoattractants. Loss of a single allele of *Rgs1* enhances chemotaxis while loss of a single allele of *Gnai2* reduced it. In contrast loss of a single allele of *Ccr7* had a very modest impact of B cell chemotaxis to a cognate ligand. Disruption of both alleles of *Rgs1* further increased chemokine induced rise in $[Ca^{2+}]_i$ and chemotaxis while loss of both

alleles of *Gnai2* markedly attenuated the responses. Disruption of a single allele of *Rgs1* and a single allele of *Gnai2* partially normalized the responses. The loss of both alleles of *Gnai2* or *Rgs1* inversely affected the number of marginal zone B cells. The architecture of the marginal zone sinuses in the spleens of the *Gnai2*$^{-/-}$ and double knock-out mice were disrupted. Further supporting the importance of *Gnai2* in B cell chemotaxis, *Gnai3*$^{-/-}$ B cells responded better than did wild type B cells to chemoattractants. Together these results argue that the ratio between RGS proteins and $G\alpha_{i2}$ also prominently affects B cell chemokine responsiveness and can affect the overall lymphoid architecture.

Our data and data from the analysis of other G-protein coupled signaling pathways support the concept that cells actively modulate intracellular signaling components to help process and transmit quantitative information about their environment. Among the best studied G-protein linked signaling pathway is a G-protein coupled receptor (GPCR)/mitogen activated protein kinase (MAPK) cascade used by haploid *Saccharomyces cerevisiae* yeast cells to sense and respond to pheromone secreted by cells of the opposite mating type. Signaling through this pathway is highly dependent upon the levels of a yeast RGS protein Sst2 and the yeast G-protein α subunit Gpa1.[28–31] Furthermore, yeast cells modulate their expression of Gpa1 and Sst2 both by transcriptional regulation and by post-translational modifications in response to pheromone. In mammalian cells RGS proteins and Gα subunits are also subject to complex regulation. In B lymphocytes RGS1 expression is regulated at the transcription level by antigen receptor engagement, toll receptor signaling, and by hypoxia.[18,19,32,33] Although not documented for RGS1 several RGS proteins are substrates of the N-end rule pathway and RGS20 undergoes ubiquitin mediated degradation as a consequence of G-protein activation.[34,35]

The failure of *Gnai3* to compensate for the loss of *Gnai2* and the modestly enhanced chemokine signaling output in the *Gnai3*$^{-/-}$ B cells was initially puzzling as $G\alpha_{i2}$ and $G\alpha_{i3}$ are often thought to be interchangeable. However, emerging data from the analysis of knock-out mice indicates that is some instances there may be little functional redundancy *in vivo*. For example, *Gnai2*$^{-/-}$ mice have a selective defect of parasympathetic modulation of heart rate not seen in *Gnai1/Gnai3* double knock-out mice.[36] Furthermore, a recent reconstitution study in Sf9 cells that showed CXCL12 induced GTPase activity in cell membrane preparations containing either $G\alpha_{i1}$ or $G\alpha_{i2}$ exceeded that noted with membranes containing $G\alpha_{i3}$ and greatly exceeded those expressing $G\alpha_{o}$ suggesting that CXCR4 preferentially couples to $G\alpha_{i1}$ and $G\alpha_{i2}$.[37] A previous study using T cells from *Gnai3* deficient T cells had noted that a greater percentage of *Gnai3*$^{-/-}$ T cells responded to CXCR3 ligands than did wild type mice, although that was not the case for the CXCR4 ligand CXCL12.[17] Ligand bound CXCR3 bound $G\alpha_{i3}$, but failed to trigger nucleotide exchange suggesting that it acted as a competitive inhibitor of $G\alpha_{i2}$.[17] Our overexpression studies using a human B cell line also have suggested that $G\alpha_{i2}$ mediates chemokine receptor signaling to chemotaxis in human B cells although they did not reveal any competitive inhibitor effect of Gαi3. (IY Hwang, unpublished data)

The opposing marginal zone B cell phenotypes of the *Rgs1* and *Gnai2* knock-mice argues that GPCR-signaling via $G\alpha_{i2}$ affects the immature B cell fate decision between follicular and marginal zone B cells. This decision is known to be influenced by extracellular inputs

delivered by the B cell antigen receptors (BCR) and Notch receptors.[27,38] A weak BCR signal predisposes immature B cells towards a marginal zone B cell phenotype while a strong signal has the opposite effect. Those immature B cells that interact with Delta-like-1 (DL1), a Notch ligand present on vascular endothelial cells in the red pulp, become marginal zone B cell precursors while those that do not become T2 cells eventually yielding follicular B cells.[38] The marginal zone B cell defect in the *Gnai2*$^{-/-}$ mice is intrinsic to lymphoid compartment as *Rag2*$^{-/-}$ mice reconstituted with *Gnai2*$^{-/-}$ bone marrow also had a reduction in marginal zone B cells.[24] Weak BCR signaling, impaired chemotaxis, or defects in T cell function were considered as possible explanations for the phenotype.[24] This study favors the second explanation. A failure of *Gnai2*$^{-/-}$ T1 B cells entering the spleen to find and interact with DL1+ endothelial cells would provide an explanation of the phenotype as it would bias the cells toward becoming follicular B cells. Conversely; an enhanced sensitivity of *Rgs1*$^{-/-}$ T1 B cells to localizing signals present in the marginal zone such as S1P[39] might bias the decision towards a marginal zone fate explaining the opposite phenotype. Besides the reduction in marginal zone B cells, the morphology of the marginal zone sinuses in the spleens of the *Gnai2*$^{-/-}$ was abnormal, resembling that previously observed in the *S1pr3*$^{-/-}$ mice.[40] Similar to those mice the MAdCAM-1^{+} endothelial cells did not form a cohesive ring around the follicle and the MOMA1^{+} macrophages were displaced from their usual positions along the sinus. The studies of the *S1pr3*$^{-/-}$ mice have indicated that the initial defect is likely a failure of the MAdCAM-1^{+} endothelial cells to properly encircle the follicle and that the mis-positioning of the MOMA1^{+} macrophages is secondary.[40] The results presented here suggest that S1pr3 signaling in these cells depends predominantly upon $G\alpha_{i2}$.

The lack of CCR7 or CXCR5 affects the splenic architecture[23,41–43] and in this study abnormal chemokine receptor signaling output was shown to impact the organization of the spleen. In the spleen most B cells likely enter into the periarteriolar lymphoid sheath (PALS) via the bridging channels.[44] A $G\alpha_i$-dependent step is needed to cross the endothelium in order to enter into the PALS.[45] CXCR5 deficient B cells enter the PALS presumably using CCR7, but cannot access the B cell zone because of failure to response to CXCL13.[41] The *Gnai2*$^{-/-}$ B cells in the spleen exhibit a complex phenotype likely a result of both reduced CCR7 and CXCR5 signaling. Many cells apparently fail to enter into the PALS and can be found in the red pulp of the spleen. Those cells that do enter the PALS will likely respond poorly to the CCR7 localizing signals and to the CXCL13 gradient that would normally trigger their movement into the B cell follicles. The net result likely explains the small B cell follicles in these mice. Cell transfer experiments examining the localization of *Gnai2*$^{-/-}$ B cells and T cells in wild type lymph nodes are consistent with these observations.[8,9] The *Gnai2*$^{-/-}$ B cells and T cells that enter lymph nodes often fail to migrate away from the cortical ridge region into their respective B cell and T cell zones. Conversely, *Rgs1*$^{-/-}$ B cells more rapidly localize in the B cell zone of lymph nodes than do wild type B cells.[8] In the *Rgs1*$^{-/-}$ mice the follicles in the spleen were more prominent than those in wild type mice likely as a consequence of the enhanced responsiveness of *Rgs1*$^{-/-}$ B cells to FDC associated CXCL13.

The proper organization of germinal centers depends upon the localization of CXCL12 in the dark zone and CXCL13 in the light zone.[46] Consistent with a need for chemokine receptor signaling for germinal center zoning the loss of *Gnai2* expression resulted in a severe disruption of the normal germinal center morphology. Modeling germinal center B cell migration predicts that chemotaxis is needed to maintain the germinal center dark and light zone, however, the B cells must down-regulate their chemokine sensitivity after transition between zones.[47] If they do not, the normal zoning of the germinal center is predicted to be disrupted. Since chemokine sensitivity is predominantly a function of chemokine receptor affinity, $G\alpha_{i2}$ levels, RGS protein expression, and receptor levels; variations in these parameters likely generate germinal center zoning. Receptor affinity is unlikely to vary during transition from centroblast to centrocyte transition arguing that the other parameters are likely more important. Centroblasts have elevated levels of CXCR4[46] and increased expression of *Rgs1* and *Rgs13* (J. Kehrl, unpublished observation) These RGS proteins may function to limit the retention of centroblasts in the dark zone and their downregulation along with decreased CXCR4 expression contribute to increased sensitivity to CXCL13. The lack of RGS1 might enhance CXCL12 signaling abnormally retaining centroblasts in the dark zone resulting in an expanded dark zone and overall germinal center size. Alternatively, RGS1 may affect signaling through another GPCR that functions in germinal center zoning.

In conclusion, the ratio between RGS1 and $G\alpha_{i2}$ in B lymphocytes impacts the sensitivity of B cells to chemoattractants. The levels of RGS1 and $G\alpha_{i2}$ are affected by environmental signals providing a mechanism by which B cells can modulate their responsiveness to chemoattractant signals independent of changes in receptor expression. The lack of RGS1 or $G\alpha_{i2}$ causes a significant alteration in lymphoid architecture and abnormal immune responses. Both B cells follicles and germinal center morphology are altered in the mutant mice. A more comprehensive understanding of chemoattractant signaling will require additional insights into how receptor input is matched to receptor output. Unraveling the mechanisms that dynamically control receptor, RGS protein, and G-protein expression should assist in this endeavor.

Material and Methods

Mice

The generation of *Gnai2*$^{-/-}$ and *Rgs1*$^{-/-}$ mice has been previously described.[8,15,25]. The mutations have been backcrossed on to a C57BL/6 background a minimum of 6 times. *Gnai2*$^{-/-}$ and *Rgs1*$^{-/-}$ mice were interbred to generate double heterozygotes. These mice were then bred to generate littermates with the desired genotypes. The *Gnai3*$^{-/-}$ mice have been previously described and have been backcrossed 3–6 generations onto a C57BL/6 background (23). The *Ccr7* targeted mice were purchased from Jackson Laboratories. All mice used in this study were 8 to 14 wk of age. Mice were housed under specific-pathogen-free conditions and used in accordance with the guidelines of the Institutional Animal Care Committee at the National Institutes of Health.

Reagents

Antibodies against mouse CD11a, CD11c, GR-1, CD4, CD8a, CD21, CD23, B220, and CCR7 were purchased from BD Pharmingen. Streptavidin conjugated to phycoerythrin was also purchased from BD Pharmingen. Murine CCL19, CXCL12, and CXCL13 were purchased from R&D Systems.

Cells

Splenic B cells were isolated by negative depletion using biotinylated antibodies to CD4, CD8, GR-1, and CDllc with Dynabeads M-280 Streptavidin (Invitrogen) as previously described.[25] The cell purity was greater than 95%. Cells were placed in complete RPMI 1640 medium supplemented with 10% FCS, 2 mM L-glutamine, 100 IU/ml penicillin, 100 μg/ml streptomycin, 1 mM sodium pyruvate, and 50 μM 2-mercaptoethanol.

Chemotaxis assays

Chemotaxis assays were performed using a transwell chamber as previously described.[25] The cells were washed twice, resuspended in complete RPMI 1640 medium and added in a volume of 100 μl to the upper wells of a 24-well transwell plate with a 5-μm insert. Lower wells contained various doses of chemokines in 600 μl of complete RPMI 1640 medium. The number of cells that migrated to the lower well following a 2-h incubation was counted using a flow cytometer. The flow cytometric analysis of receptor expression was performed on a FACSCanto II flow cytometer (BD Biosciences) and the data were analyzed using the FlowJo software (Tree Star, Inc.). Forward and side scatter parameters were used to gate on live cells.

Changes in $[Ca^{2+}]_i$

Cells were seeded at 10^5 cells per 100 μl loading medium (RPMI 1640, 10% FBS) into poly-D-lysine coated 96-well black wall, clear-bottom microtiter plates (Nalgene Nunc). An equal volume of assay loading buffer (FLIPR Calcium 3 assay kit, Molecular Devices) in Hank's balanced salt solution supplemented with 20 mM HEPES and 2 mM probenecid was added. Cells were incubated for 1 h at 37 °C before adding chemokine and then the calcium flux peak was measured using a FlexStation 3 (Molecular Devices). The data was analyzed with SOFT max Pro 5.2 (Molecular Devices). Data is shown as fluorescent counts and the y-axis labeled as Lm1. In some instances the data was imported into Graph Pad Prism 5 (GraphPad Software) and the log concentration of chemokine plotted versus the maximum response. The dose response curve generated using a non-linear fit of the data.

Immunohistochemistry

Freshly isolated spleens were snap frozen in Tissue-Tek OCT compound (Sakura Finetek). Frozen OCT splenic sections (7 μm) were acetone fixed for 2 min, and dried at room temperature. Slides were rehydrated in Tris-buffered saline (TBS) and stained in a humidified chamber in TBS/0.1% BSA/1% mouse serum overnight at 4 °C or 1 h at room temperature. Primary antibodies included rat anti-mouse CD45R (RA3-6B2, purified; BD Pharmingen) and Armenian hamster anti-mouse CD3e (145-2C11, purified; BD Pharmingen). Also used were PNA lectin (biotinylated; Sigma), rat anti-mouse IgD (11–26c.

2a, purified; BD Pharmingen), rat anti-mouse CD35 (8C12, biotinylated BD Pharmingen), rat anti-mouse CD1d (1B1, biotinylated; BD Pharmingen), rat anti-mouse mAb CD169 (MOMA-1, purified; Serotec), rat anti-mouse MAdCAM-1 (MECA-367, purified; BD Pharmingen). Biotinylated antibodies were detected with streptavidin-alkaline phosphatase (Jackson ImmunoResearch Laboratories), and purified mAbs with AP conjugated goat anti-Armenian hamster IgG (H+L) (Jackson ImmunoResearch Laboratories) or HRP conjugated donkey anti-rat IgG (H+L) (Jackson ImmunoResearch Laboratories). HRP was reacted with DAB (Peroxidase Substrate Kit; Vector), and alkaline phosphatase with Fast Blue/Napthol AS-MX; Sigma-Aldrich). Levamisole (Sigma-Aldrich) was used to block endogenous alkaline phosphatase activity. Slides were mounted in Crystal Mount (Electron Microscopy Sciences). For immunofluorescence, frozen acetone fixed section were stained with a mixture of FITC-conjugated $F(ab')_2$ goat anti-mouse IgM and rat anti IgD (11–26c.2a, purified; BD Pharmingen), 4 °C overnight. The IgD was detected with Rhodamine Red-X-conjugated $F(ab')_2$ donkey anti-rat (Jackson ImmunoResearch). Slides were mounted with Vectashield (Vector Labs). Images were acquired either with an Olympus BX-50 microscope equipped with a ProgRes-digital microscope camera (Jenoptik) or a Zeiss Axiovert 200 fluorescent microscope equipped with a Sensicam EM camera (Cooke). The number of germinal centers per spleen section was determined by Immunostaining with PNA/B220 or IgD/CD3 multiple splenic sections from two mice of each genotype.

Statistics

Results represent samples from 3–6 mice per experiment. All experiments were performed more than three times unless noted. All statistical analysis was performed with GraphPad Prism (GraphPad Software). Significance of statistics was calculated with unpaired t test for two nonparametric data and with Kruskal-Wallis test for three nonparametric data. A chi-square test for genotype was used to measure the association between observed each genotype numbers versus expected genotype numbers.

Acknowledgments

The authors would like than Mary Rust for excellent editorial assistance and Dr. Anthony Fauci for his continued support. This research was supported by the Intramural Research Program of the National Institute of Allergy and Infectious Diseases, National Institutes of Health.

References

1. Springer TA. Traffic signals for lymphocyte recirculation and leukocyte emigration: the multistep paradigm. Cell. 1994; 76(2):301–314. [PubMed: 7507411]
2. Kunkel EJ, Butcher EC. Chemokines and the tissue-specific migration of lymphocytes. Immunity. 2002; 16(1):1–4. [PubMed: 11825560]
3. Cyster JG. Chemokines, sphingosine-1-phosphate, and cell migration in secondary lymphoid organs. Annu Rev Immunol. 2005; 23:127–159. [PubMed: 15771568]
4. Neptune ER, Bourne HR. Receptors induce chemotaxis by releasing the betagamma subunit of Gi, not by activating Gq or Gs. Proc Natl Acad Sci U S A. 1997; 94(26):14489–14494. [PubMed: 9405640]
5. Arai H, Tsou CL, Charo IF. Chemotaxis in a lymphocyte cell line transfected with C-C chemokine receptor 2B: evidence that directed migration is mediated by betagamma dimers released by activation of Galphai-coupled receptors. Proc Natl Acad Sci U S A. 1997; 94(26):14495–14499. [PubMed: 9405641]

6. Hepler JR, Gilman AG. G proteins. Trends Biochem Sci. 1992; 17(10):383–387. [PubMed: 1455506]
7. Neer EJ. Heterotrimeric G proteins: organizers of transmembrane signals. Cell. 1995; 80(2):249–257. [PubMed: 7834744]
8. Han SB, Moratz C, Huang NN, Kelsall B, Cho H, Shi CS, et al. Rgs1 and Gnai2 regulate the entrance of B lymphocytes into lymph nodes and B cell motility within lymph node follicles. Immunity. 2005; 22(3):343–354. [PubMed: 15780991]
9. Hwang IY, Park C, Kehrl JH. Impaired trafficking of Gnai2+/− and Gnai2−/− T lymphocytes: implications for T cell movement within lymph nodes. J Immunol. 2007; 179(1):439–448. [PubMed: 17579064]
10. Wettschureck N, Moers A, Offermanns S. Mouse models to study G-protein-mediated signaling. Pharmacol Ther. 2004; 101(1):75–89. [PubMed: 14729394]
11. Jin Y, Wu MX. Requirement of Galphai in thymic homing and early T cell development. Mol Immunol. 2008; 45(12):3401–3410. [PubMed: 18501427]
12. Kinzer-Ursem TL, Linderman JJ. Both ligand- and cell-specific parameters control ligand agonism in a kinetic model of g protein-coupled receptor signaling. PLoS Comput Biol. 2007; 3(1):e6. [PubMed: 17222056]
13. Kehrl JH. Heterotrimeric G protein signaling: roles in immune function and fine-tuning by RGS proteins. Immunity. 1998; 8(1):1–10. [PubMed: 9462506]
14. Zhong H, Neubig RR. Regulator of G protein signaling proteins: novel multifunctional drug targets. J Pharmacol Exp Ther. 2001; 297(3):837–845. [PubMed: 11356902]
15. Rudolph U, Finegold MJ, Rich SS, Harriman GR, Srinivasan Y, Brabet P, et al. Ulcerative colitis and adenocarcinoma of the colon in G alpha i2-deficient mice. Nat Genet. 1995; 10(2):143–150. [PubMed: 7663509]
16. Gohla A, Klement K, Piekorz RP, Pexa K, vom Dahl S, Spicher K, et al. An obligatory requirement for the heterotrimeric G protein Gi3 in the antiautophagic action of insulin in the liver. Proc Natl Acad Sci U S A. 2007; 104(8):3003–3008. [PubMed: 17296938]
17. Thompson BD, Jin Y, Wu KH, Colvin RA, Luster AD, Birnbaumer L, et al. Inhibition of G alpha i2 activation by G alpha i3 in CXCR3-mediated signaling. J Biol Chem. 2007; 282(13):9547–9555. [PubMed: 17289675]
18. Moratz C, Kang VH, Druey KM, Shi CS, Scheschonka A, Murphy PM, et al. Regulator of G protein signaling 1 (RGS1) markedly impairs Gi alpha signaling responses of B lymphocytes. J Immunol. 2000; 164(4):1829–1838. [PubMed: 10657631]
19. Shi GX, Harrison K, Han SB, Moratz C, Kehrl JH. Toll-like receptor signaling alters the expression of regulator of G protein signaling proteins in dendritic cells: implications for G protein-coupled receptor signaling. J Immunol. 2004; 172(9):5175–5184. [PubMed: 15100254]
20. Han JI, Huang NN, Kim DU, Kehrl JH. RGS1 and RGS13 mRNA silencing in a human B lymphoma line enhances responsiveness to chemoattractants and impairs desensitization. J Leukoc Biol. 2006; 79(6):1357–1368. [PubMed: 16565322]
21. Bansal G, DiVietro JA, Kuehn HS, Rao S, Nocka KH, Gilfillan AM, et al. RGS13 controls g protein-coupled receptor-evoked responses of human mast cells. J Immunol. 2008; 181(11):7882–7890. [PubMed: 19017978]
22. Sinha RK, Park C, Hwang IY, Davis MD, Kehrl JH. B lymphocytes exit lymph nodes through cortical lymphatic sinusoids by a mechanism independent of sphingosine-1-phosphate-mediated chemotaxis. Immunity. 2009; 30(3):434–446. [PubMed: 19230723]
23. Reif K, Ekland EH, Ohl L, Nakano H, Lipp M, Forster R, et al. Balanced responsiveness to chemoattractants from adjacent zones determines B-cell position. Nature. 2002; 416(6876):94–99. [PubMed: 11882900]
24. Dalwadi H, Wei B, Schrage M, Spicher K, Su TT, Birnbaumer L, et al. B cell developmental requirement for the G alpha i2 gene. J Immunol. 2003; 170(4):1707–1715. [PubMed: 12574334]
25. Moratz C, Hayman JR, Gu H, Kehrl JH. Abnormal B-cell responses to chemokines, disturbed plasma cell localization, and distorted immune tissue architecture in Rgs1−/− mice. Mol Cell Biol. 2004; 24(13):5767–5775. [PubMed: 15199133]

26. Allen CD, Cyster JG. Follicular dendritic cell networks of primary follicles and germinal centers: phenotype and function. Semin Immunol. 2008; 20(1):14–25. [PubMed: 18261920]
27. Martin F, Kearney JF. Marginal-zone B cells. Nat Rev Immunol. 2002; 2(5):323–335. [PubMed: 12033738]
28. Hao N, Yildirim N, Wang Y, Elston TC, Dohlman HG. Regulators of G protein signaling and transient activation of signaling: experimental and computational analysis reveals negative and positive feedback controls on G protein activity. J Biol Chem. 2003; 278(47):46506–46515. [PubMed: 12968019]
29. Wang Y, Marotti LA Jr, Lee MJ, Dohlman HG. Differential regulation of G protein alpha subunit trafficking by mono- and polyubiquitination. J Biol Chem. 2005; 280(1):284–291. [PubMed: 15519996]
30. Behar M, Hao N, Dohlman HG, Elston TC. Mathematical and computational analysis of adaptation via feedback inhibition in signal transduction pathways. Biophys J. 2007; 93(3):806–821. [PubMed: 17513354]
31. Yu RC, Pesce CG, Colman-Lerner A, Lok L, Pincus D, Serra E, et al. Negative feedback that improves information transmission in yeast signalling. Nature. 2008; 456(7223):755–761. [PubMed: 19079053]
32. Reif K, Cyster JG. RGS molecule expression in murine B lymphocytes and ability to down-regulate chemotaxis to lymphoid chemokines. J Immunol. 2000; 164(9):4720–4729. [PubMed: 10779778]
33. Piovan E, Tosello V, Indraccolo S, Masiero M, Persano L, Esposito G, et al. Differential regulation of hypoxia-induced CXCR4 triggering during B-cell development and lymphomagenesis. Cancer Res. 2007; 67(18):8605–8614. [PubMed: 17875700]
34. Lee MJ, Tasaki T, Moroi K, An JY, Kimura S, Davydov IV, et al. RGS4 and RGS5 are in vivo substrates of the N-end rule pathway. Proc Natl Acad Sci U S A. 2005; 102(42):15030–15035. [PubMed: 16217033]
35. Pagano M, Jordan JD, Neves SR, Nguyen T, Iyengar R. Galphao/i-stimulated proteosomal degradation of RGS20: a mechanism for temporal integration of Gs and Gi pathways. Cell Signal. 2008; 20(6):1190–1197. [PubMed: 18407463]
36. Zuberi Z, Birnbaumer L, Tinker A. The role of inhibitory heterotrimeric G proteins in the control of in vivo heart rate dynamics. Am J Physiol Regul Integr Comp Physiol. 2008; 295(6):R1822–1830. [PubMed: 18832081]
37. Kleemann P, Papa D, Vigil-Cruz S, Seifert R. Functional reconstitution of the human chemokine receptor CXCR4 with G(i)/G (o)-proteins in Sf9 insect cells. Naunyn Schmiedebergs Arch Pharmacol. 2008; 378(3):261–274. [PubMed: 18523757]
38. Tan JB, Xu K, Cretegny K, Visan I, Yuan JS, Egan SE, et al. Lunatic and manic fringe cooperatively enhance marginal zone B cell precursor competition for delta-like 1 in splenic endothelial niches. Immunity. 2009; 30(2):254–263. [PubMed: 19217325]
39. Cinamon G, Matloubian M, Lesneski MJ, Xu Y, Low C, Lu T, et al. Sphingosine 1-phosphate receptor 1 promotes B cell localization in the splenic marginal zone. Nat Immunol. 2004; 5(7): 713–720. [PubMed: 15184895]
40. Girkontaite I, Sakk V, Wagner M, Borggrefe T, Tedford K, Chun J, et al. The sphingosine-1-phosphate (S1P) lysophospholipid receptor S1P3 regulates MAdCAM-1+ endothelial cells in splenic marginal sinus organization. J Exp Med. 2004; 200(11):1491–1501. [PubMed: 15583019]
41. Forster R, Mattis AE, Kremmer E, Wolf E, Brem G, Lipp M. A putative chemokine receptor, BLR1, directs B cell migration to defined lymphoid organs and specific anatomic compartments of the spleen. Cell. 1996; 87(6):1037–1047. [PubMed: 8978608]
42. Forster R, Schubel A, Breitfeld D, Kremmer E, Renner-Muller I, Wolf E, et al. CCR7 coordinates the primary immune response by establishing functional microenvironments in secondary lymphoid organs. Cell. 1999; 99(1):23–33. [PubMed: 10520991]
43. Ansel KM, Ngo VN, Hyman PL, Luther SA, Forster R, Sedgwick JD, et al. A chemokine-driven positive feedback loop organizes lymphoid follicles. Nature. 2000; 406(6793):309–314. [PubMed: 10917533]

44. Bajenoff M, Glaichenhaus N, Germain RN. Fibroblastic reticular cells guide T lymphocyte entry into and migration within the splenic T cell zone. J Immunol. 2008; 181(6):3947–3954. [PubMed: 18768849]

45. Cyster JG, Goodnow CC. Pertussis toxin inhibits migration of B and T lymphocytes into splenic white pulp cords. J Exp Med. 1995; 182(2):581–586. [PubMed: 7629515]

46. Allen CD, Ansel KM, Low C, Lesley R, Tamamura H, Fujii N, et al. Germinal center dark and light zone organization is mediated by CXCR4 and CXCR5. Nat Immunol. 2004; 5(9):943–952. [PubMed: 15300245]

47. Figge MT, Garin A, Gunzer M, Kosco-Vilbois M, Toellner KM, Meyer-Hermann M. Deriving a germinal center lymphocyte migration model from two-photon data. J Exp Med. 2008; 205(13): 3019–3029. [PubMed: 19047437]

48. Jiang M, Spicher K, Boulay G, Wang Y, Birnbaumer L. Most central nervous system D2 dopamine receptors are coupled to their effectors by Go. Proc Natl Acad Sci U S A. 2001; 98(6):3577–3582. [PubMed: 11248120]

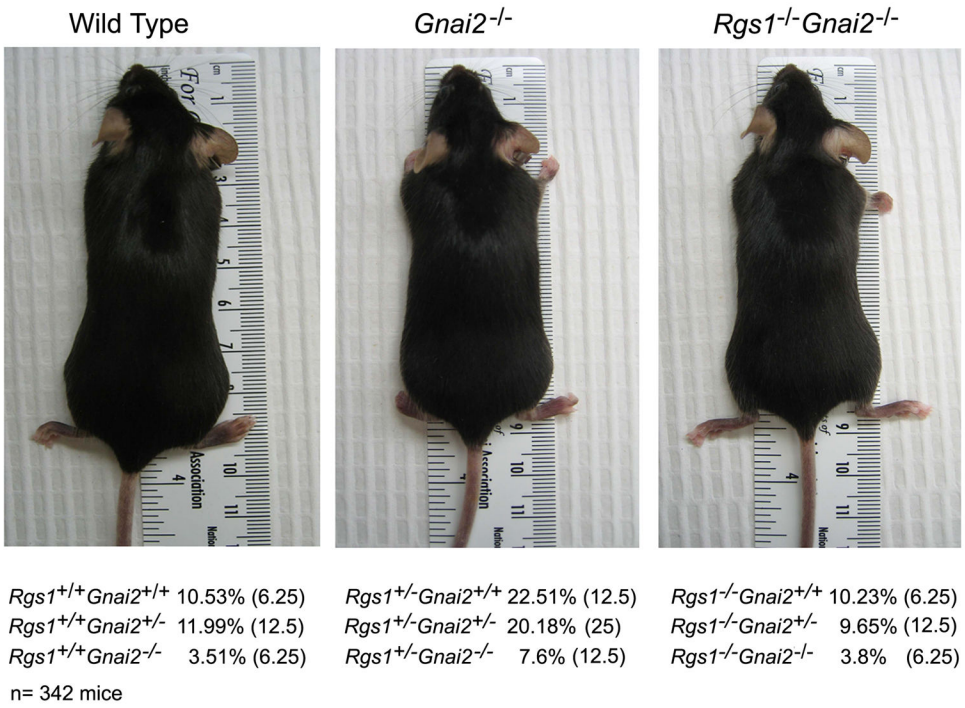

Figure 1.

Intercross of *Rgs1*$^{+/-}$ and *Gnai2*$^{+/-}$ mice. Photographs of representative wild type, *Gnai2*$^{-/-}$, and *Rgs1*$^{-/-}$/*Gnai2*$^{-/-}$ C57/BL6 mice. The result of genotyping mice from double heterozygote crosses is shown below the photographs. The percentage of each of the different genotypes is shown and in parentheses the predicted frequency of the genotype. The results are from genotyping 342 mice. The p values are significantly different for each observed genotype number vs. expected genotype number ($P < 0.001$ by chi-square tests).

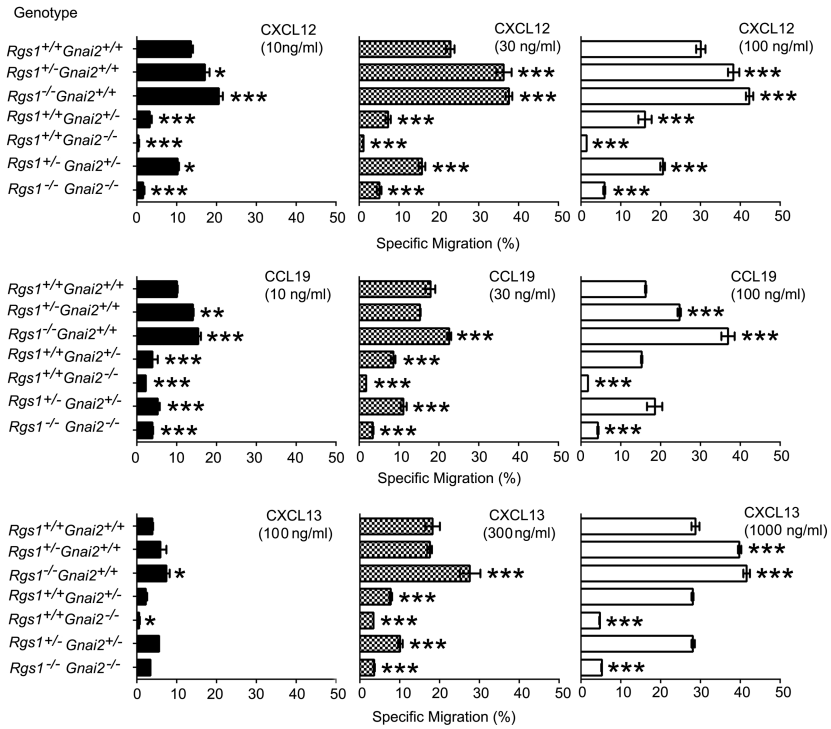

Figure 2.

Comparison of B cells prepared from the different genotypes in standard chemotaxis assays. B cells purified from wild-type and mice with varying intact alleles of *Rgs1* and *Gnai2* were subjected to a 2 h chemotaxis in response to different concentrations of CXCL12, CCL19, or CXCL13 as indicated. The percentages of cells responding to are shown. Results are mean and standard error of sextuplet samples from four experiments and are shown as % specific migration. Statistical significance was calculated using Mann-Whitney t-test compared with $Rgs1^{+/+}Gnai2^{+/+}$. (*, $p<0.05$, **, $p<0.01$, and ***, $p<0.001$) Specific migration is the percentage cells responding to chemokine minus the percentage cells that spontaneously migrate in the absence of chemokine.

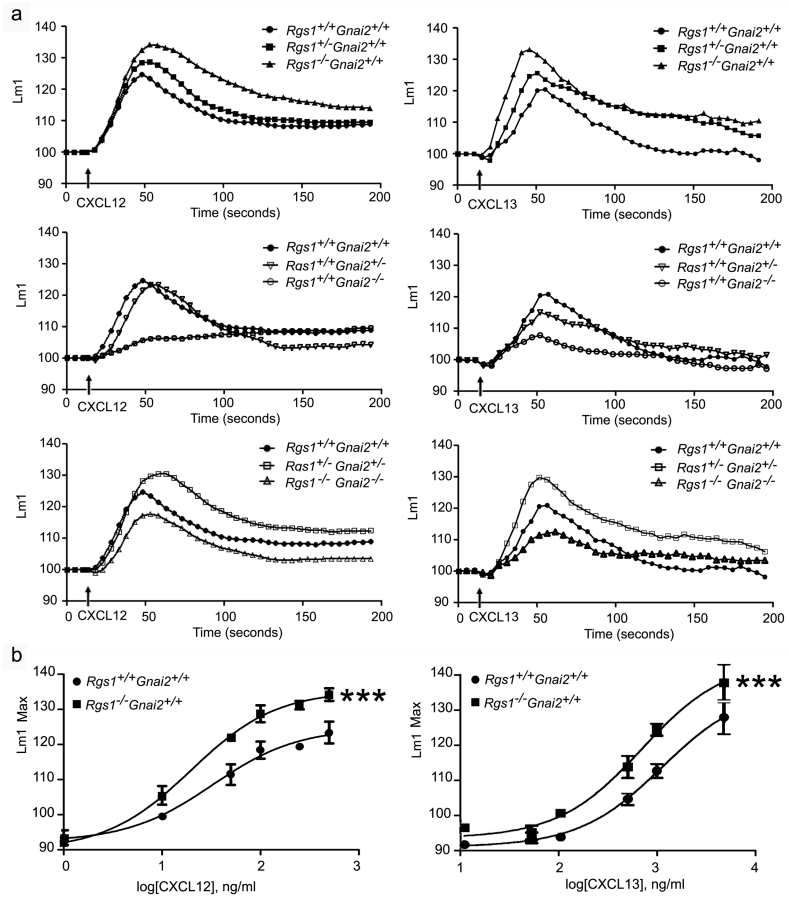

Figure 3.

Measurement of changes in $[Ca^{+2}]_i$ stimulated by chemokine exposure. A. Comparison of B cells from different mice. B cells purified from the spleens of wild type and mice with varying alleles of *Rgs1* and *Gnai2* were prepared and then incubated for 1 h at 37°C in the calcium assay loading buffer before adding CXCL12 or CXCL13 (100 or 1000 ng/ml, respectively). Changes in $[Ca^{+2}]_i$ were monitored over 3 min. The data was analyzed with SOFT max Pro 5.2 and is shown as fluorescent counts and the y-axis labeled as Lm1. Each experimental value is the mean of three determinations. The experiment was performed three times with similar results. B. Comparison of $[Ca^{+2}]_i$ stimulated by different chemokine concentrations with wild type or *Rgs1*$^{-/-}$ B cells. Wild type or *Rgs1*$^{-/-}$ B cells were stimulated with increasing concentrations of CXCL12 or CXCL13 as indicated. The data was analyzed with SOFT max Pro 5.2 and transformed with Graph Pad Prism and a linear regression analysis performed to fit the curves. Each experimental value is the mean of three determinations. The experiment was performed three times with similar results. Statistical significance was calculated using Mann-Whitney t-test compared with wild type (*Rgs1*$^{+/+}$*Gnai2*$^{+/+}$), (*, $p<0.0001$).

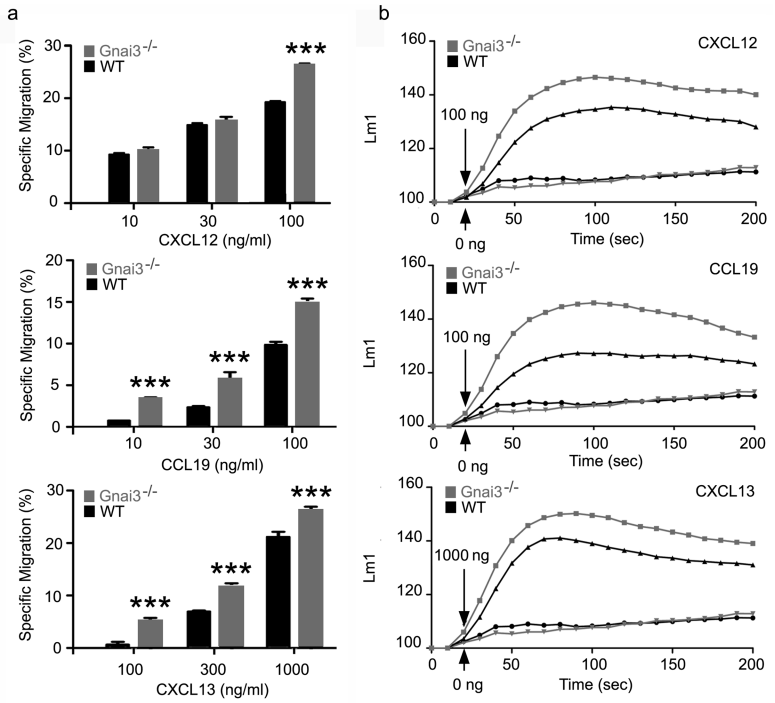

Figure 4.

Comparison of chemokine responses of B cells prepared from wild type and *Gnai3*$^{-/-}$ mice. A. Chemotaxis assays. B cells purified from wild-type (littermate controls) and *Gnai3*$^{-/-}$ mice were subjected to a 2 h chemotaxis in response to different concentrations of CXCL12, CCL19, or CXCL13 as indicated. Results are mean and standard error of sextuplet samples from three experiments and are shown as % specific migration. Statistical significance was calculated using Mann-Whitney t-test compared with *Rgs1*$^{+/+}$*Gnai2*$^{+/+}$. (***, $p<0.001$) B. Measurement of changes in $[Ca^{+2}]_i$. B cells purified from the spleens of wild type (littermate controls) and *Gnai3*$^{-/-}$ mice were prepared and incubated for 1 h at 37°C in the calcium assay loading buffer before adding CXCL12, CCL19, or CXCL13 (100, 100, or 1000 ng/ml, respectively). Changes in $[Ca^{+2}]_i$ were monitored over 3 min. The data was analyzed with SOFT max Pro 5.2 and is shown as fluorescent counts and the y-axis labeled as Lm1. Each experimental value is the mean of three determinations. The experiment was performed three times with similar results.

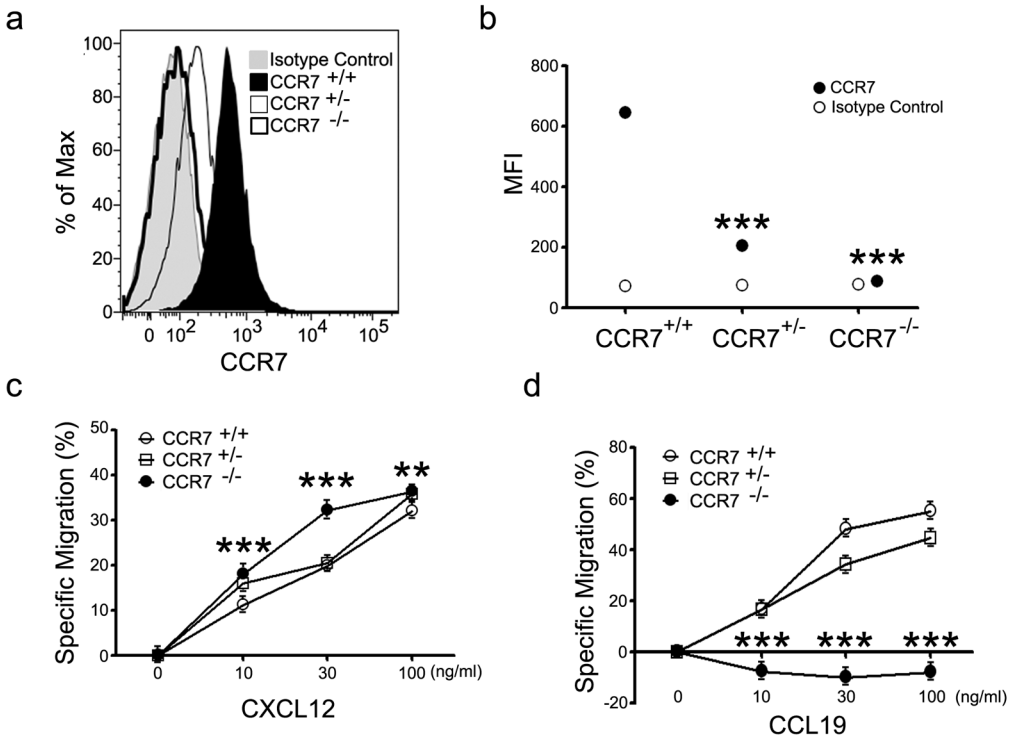

Figure 5.

Comparison of Ccl19 triggered chemotaxis of B cells from wild type, $Ccr7^{+/-}$, and $Ccr7^{-/-}$ mice. (a) CCR7 expression on wild type and mutant mice. Flow cytometry with an isotype control and CCR7 antibody. Spleens B cells were purified from wild type, $Ccr7^{+/-}$, and $Ccr7^{-/-}$ mice. Results are representative of 4 experiments done. (b) Mean Fluorescent intensity (MFI) of CCR7 expression on B cells from wild type and mutant mice. Data representative of one of four experiments performed. Statistical significance was calculated using Mann-Whitney t-test compared with MFI of CCR7 of $CCR7^{+/+}$. (***, $p<0.0001$) (c) CXCL12 mediated Chemotaxis. A standard chemotaxis assay was performed with splenic B cells. The results are mean and standard error of sextuplet samples from one experiment and are shown as % specific migration. A standard chemotaxis assay was performed with splenic B cells. Results are representative of one of 3 experiments performed. Statistical significance was calculated using Mann-Whitney t-test compared with $CCR7^{+/+}$. (**, $p<0.01$ and ***, $p<0.001$) (d) CXCL19 mediated chemotaxis. The Results are mean and standard error of sextuplet samples from one experiment and are shown as % specific migration. Results are representative of one of 3 experiments performed. Statistical significance was calculated using Mann-Whitney t-test compared with $CCR7^{+/+}$. (***, $p<0.001$)

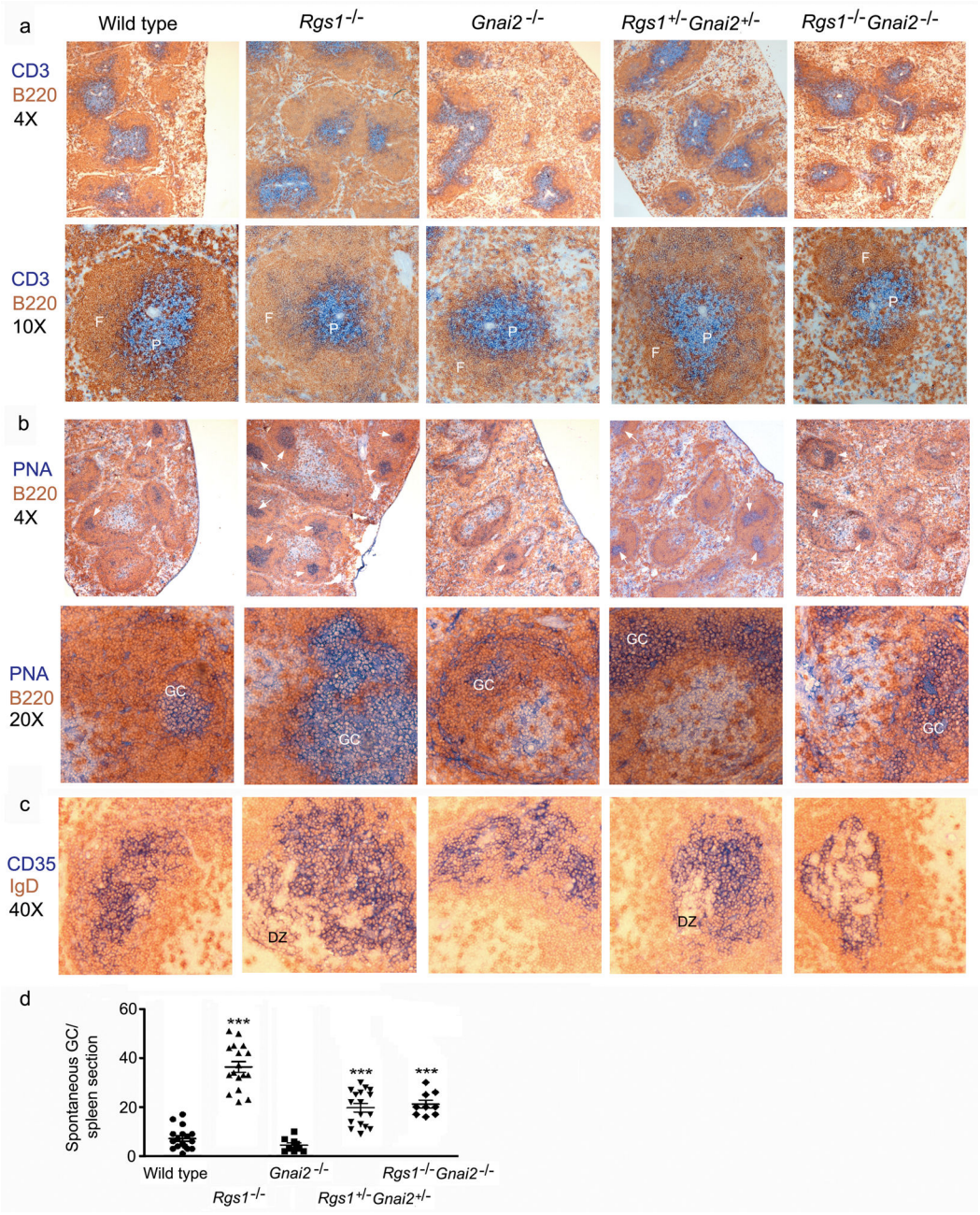

Figure 6.

Immunohistochemistry of spleens from wild type, *Rgs1*$^{-/-}$, *Gnai2*$^{-/-}$, double heterozygotic, and double knock-out mice. (a) Immunostaining CD3 versus B220. Spleens from mice with varying numbers of intact *Rgs1* and *Gnai2* alleles were immunostained for CD3 (blue) and B220 (brown). Top images show representative regions of the spleens photographed with a 4X objective. Bottom images show a single spleen follicle photographed with a 10X objective. Splenic follicle (F) and PALS (P) are denoted in each image. (b) PNA versus B220 immunostaining. Spleens from mice with varying numbers of intact *Rgs1* and *Gnai2* alleles were stained for PNA (blue) and immunostained for B220 (brown). Top images show representative regions of the spleens photographed with a 4X objective. Germinal centers

indicated with white arrow. Bottom images show a germinal center within a splenic follicle photographed with a 20X objective. Germinal centers (GC) are denoted in each image. (c) Immunostaining CD35 versus IgD. Spleens from mice with varying numbers of intact *Rgs1* and *Gnai2* alleles were immunostained for CD35 (blue) and IgD (brown). Images show germinal center within splenic follicle photographed with a 40X objective. Dark zone (DZ) region of the germinal centers are indicated. 2 sets of littermates were examined with similar results. (d) Spontaneous germinal center formation. Splenic sections immunostained with PNA versus B220. The numbers of germinal centers per spleen section from each genotype were counted. Results are from three mice of each genotype. Statistical significance was calculated using Mann-Whitney t-test compared with wt. (***, $p<0.0001$)

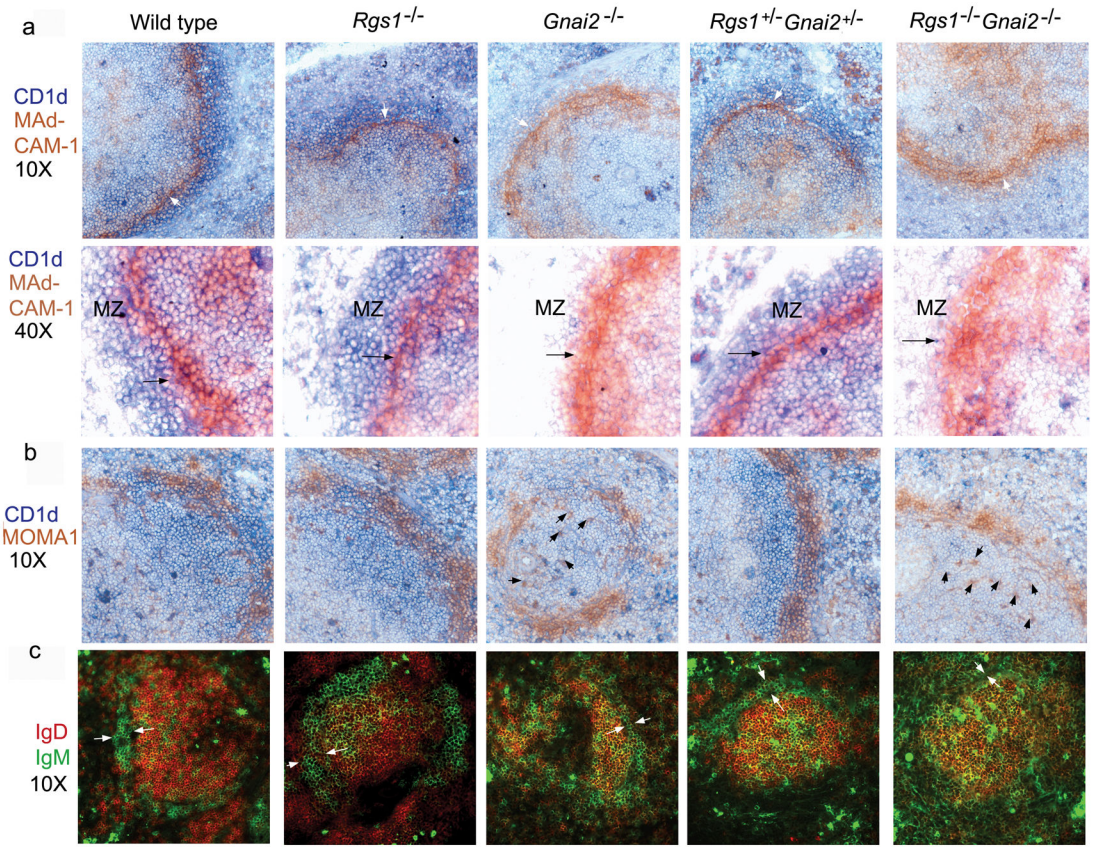

Figure 7.

Immunohistochemistry of marginal zone region in spleens from wild type, *Rgs1*$^{-/-}$, *Gnai2*$^{-/-}$, double heterozygotic, and double knock-out mice. (a) Immunostaining CD1d versus MAdCAM-1. Spleens from mice with varying numbers of intact *Rgs1* and *Gnai2* alleles were immunostained for CD1d (blue) and MAdCAM-1 (brown) and photographed with a 10X objective (top images). Marginal sinus indicated with white arrow. Bottom images show marginal zone region photographed with a 40X objective. Marginal zone region indicated and the marginal zone sinus denoted with a black arrow. (b) Immunostaining CD1d versus MOMA1. Spleens from mice with varying numbers of intact *Rgs1* and *Gnai2* alleles were immunostained for CD1d (blue) and MOMA1 (brown) and photographed with a 10X objective. Displaced MOMA-1 positive cells indicated with black arrows in the images from the *Gnai2*$^{-/-}$ and *Rgs1*$^{-/-}$*Gnai2*$^{-/-}$ mice. (c) Immunostaining IgD versus IgM. Spleens from mice with varying numbers of intact *Rgs1* and *Gnai2* alleles were immunostained for IgD (red) and IgM (green), visualized with a fluorescent microscope, and photographed with a 10X objective. Marginal zone region indicated with two white arrows in each section. 2 sets of littermates were examined with similar results.

Table 1

B cell populations in the spleen

Genotype	B220	Follicular	Transitional	Marginal Zone
Rgs1$^{+/+}$*Gnai2*$^{+/+}$	54+/− 9	72+/− 7	10+/− 0	10+/− 4
Rgs1$^{+/-}$*Gnai2*$^{+/+}$	47+/− 1	75+/− 1	6 +/− 0***	15+/− 0*
Rgs1$^{-/-}$*Gnai2*$^{+/+}$	44+/− 3*	69+/− 6	6+/− 1***	19+/− 3**
Rgs1$^{+/+}$*Gnai2*$^{+/-}$	48+/− 7	72+/− 6	8+/− 1**	12+/− 2
Rgs1$^{+/+}$*Gnai2*$^{-/-}$	44+/− 3*	74+/− 7	6+/− 2**	5+/− 2*
Rgs1$^{+/-}$*Gnai2*$^{+/-}$	42+/− 7*	68+/− 7	7+/− 1***	17+/− 3*
Rgs1$^{-/-}$*Gnai2*$^{-/-}$	52+/− 4	81+/− 4*	4+/− 1***	8+/− 3
Rgs1$^{+/+}$*Gnai3*$^{-/-}$	54+/−4	76+/−3	10+/−1	9+/−2

Percentage of B220^{+} cells, follicular B cells, transitional B cells, and marginal zone B cells found in the spleen of the different types of mice. Results are mean plus or minus 2 standard deviations of the mean of 5 mice for each genotype. Statistical significance was calculated using Mann-Whitney t-test compared with Rgs1$^{+/+}$Gnai2$^{+/+}$.

* $p<0.05$,

** $p<0.001$, and

*** $p<0.0001$